6ICEGE 6th International Conference on Earthquake Geotechnical Engineering
1-4 November 2015
Christchurch, New Zealand

PRENOLIN Project: A Benchmark on Numerical Simulation of 1D Non-Linear Site Effect. 1 – Verification Phase Based on Canonical Cases

J. Régnier[1], L.F. Bonilla[2], P.Y. Bard[3], H. Kawase[4], E. Bertrand[5], F. Hollender[6], M. Marot[7] and D. Sicilia[8]

ABSTRACT

One of the objectives of the PRENOLIN project is the assessment of uncertainties associated with non-linear simulation of 1D site effects. An international benchmark is underway to test several numerical codes, including various non-linear soil constitutive models, to compute the non-linear seismic site response. A preliminary verification phase (i.e. comparison between numerical codes) on simple and idealistic cases has been performed on 23 different codes. It is followed by a validation phase, which compares predictions of such numerical estimations with actual strong motion data recorded from well-known sites. The verification was initially conducted on elastic and visco-elastic computations to ensure a common understanding of the parameters and identical results. Then, the non-linear results provide a quantification of the epistemic uncertainties linked to wave propagation modeling using different non-linear rheological models. PRENOLIN is part of two larger projects: SINAPS@, funded by the ANR (French National Research Agency) and SIGMA, funded by a consortium of nuclear operators (EDF, CEA, AREVA, ENL).

Introduction

While a consensus has undoubtedly been reached on the existence of non-linear effects, their quantification and modeling remain a challenge, despite the existence of a commonly accepted practice. The ability to accurately predict non-linear site responses has indeed already been the subject of two recent comparative tests. It was one of the targets of the pioneering blind tests initiated in the late 80's/early 90's on 2 sites, Ashigara Valley (Japan) and Turkey Flat (California); however, those sites lacked strong motion records until the 2004 Parkfield earthquake, during which the Turkey Flat site experienced a 0.3g motion. A new benchmarking of 1D non-linear codes was since carried out in the last decade. Its main findings were reported by (Kwok et al., 2008) and (Stewart and Kwok, 2009)), who emphasized the key importance of the way these codes are used and the required in-situ measurements. Tests using 2D modeling were also performed (Cashima/E2VP project), but the geometrical complexity did not allow to

[1]Régnier Julie, CEREMA, Nice, France, Julie.regnier@cerema.fr
[2]Bonilla Luis-Fabian, IFSTTAR, Paris, France, fabian.bonilla @ifsttar.fr
[3]Bard Pierre-Yves, IsTerre, Grenoble, France, pierre-yves.bard@ujf-grenoble.fr
[4]Kawase Hirosho, DPRI, Kyoto, Japan, kawase.hiroshi.6x@kyoto-u.ac.jp
[5]Bertrand Etienne, CEREMA, Nice, France, etienne.bertrand@cerema.fr
[6]Hollender Fabrice, CEA, Cadarache, France, fabrice.hollender@cea.fr
[7]Marot Marianne, CEREMA, Nice, France, marianne.marot@hotmail.com
[8]Sicillia Deborah, EDF, Aix-en-Provence, France, deborah.sicilia@edf.fr

deeply analyze the implementation of the non-linear soil behavior. For this reason, the PRENOLIN project considers only 1D soil columns to test the non-linear codes in the simplest possible, though realistic, geometries. It is organized in two phases: (1) the initial verification phase, aiming at a cross-code comparison on very simple idealistic 1D soil columns with prescribed linear and non-linear parameters; (2) The subsequent validation phase, comparing numerical predictions with actual observations.

The purpose of this article is to show the results of the first phase, that is the verification, and to concentrate our attention on the epistemic uncertainties associated with the constitutive laws and numerical schemes of the simulation codes. The verification phase compares surface motions computed by different numerical codes for simple soil column configurations, and which are later compared with predefined analytical solutions, in the linear and elastic and visco-elastic domain. Similarity in the results would ensure a common understanding of the physical soil parameters to be used and a proper predictability of the induced deformation, considering various soil properties and seismic wavefield properties (amplitude, frequency content, etc). In the non-linear domain, the observed discrepancies between the different computations help identify the issues of these models and quantify the epistemic uncertainty linked to the choice of the constitutive law, numerical schemes, input motion and non-linear soil property implementations.

Proposed Canonical Cases

The verification phase experiment was devised around three 1D canonical cases, chosen to represent simple and idealistic soil conditions overlying rigid bedrock substrata; however, varying in complexity:

1) Profile 1 (P1): A homogeneous soil layer of 20 m thickness presenting significant velocity contrast with Vs equal to 300 and 2000 m/s for the soft and sediment layers respectively. The amplification effects occur at the intermediate frequency range of 2-10 Hz.
2) Profile 2 (P2): A soil layer of 100 m thickness with a positive vertical velocity gradient (from 150 m/s at the surface to 500 m/s at the soil-bedrock interface) leading to significant amplification at frequencies below 1 Hz.
3) Profile 3 (P3): Two homogeneous layers of 20 and 30 m thickness with significant velocity contrasts with Vs equal to 300, 600 and 2000 m/s for the first two soft layers and sediment layers respectively. It was constructed to investigate non-linearity effects within both layers (amplification effects begin around 2.5 Hz), since significant strains can develop at or near each interface.

P-wave speed was computed from Vs profiles using a Poisson ratio of 0.4 for soil and 0.3 for bedrock. The density is equal to 2000 kg/m3 for the soft layer and 2500 kg/m3 for the substratum. Attenuation parameters were constrained to vary according to Vs, using the classical $Q = Vs/10$ or equivalent $\xi = 5/Vs$ relationships (although never actually justified; (Olsen et al., 2003). The shear strength of the soil was not provided.

The non-linear soil properties provided are classical curves of degradation of the shear modulus, $G/Gmax(\gamma)$, and increase of the damping, $D(\gamma)$, describing the rheological behavior of each layer per profile. It does not represent a complete description of the nonlinear behavior it is restricted to shear deformation and volumetric ones and coupling between both are ignored. The shear

strength

The G/Gmax(γ) and D(γ) curves were constructed following a simple hyperbolic model and where calculated using the soil properties at the middle of each soil layers. Therefore, only one G/Gmax(γ) curve is given for one soil layer independently of the depth.

The reference input motions consist of a Ricker pulse (with central frequency of 4Hz) and two real accelerograms of high and low frequency contents (with central frequencies of 11.4 and 4.8 Hz respectively), each scaled to three PGA levels (0.05, 0.1 and 0.5 m/s^2), in order to generate a wide range of shear strain levels in the soil column. They were placed at the base of the soil column (at the sediment/bedrock interface) to assess the soil responses. And finally, two boundary conditions at the sediment/bedrock interface were tested, elastic and rigid. Rigid condition was used because for the next stage of validation down-hole recordings will be used as reference motion.

Participants and Tested Numerical Code

We compared 21 different numerical codes used by 21 participating teams. Two or more teams used the same code: SeismoSoil (A-0), FLIP (B-0), PSNL (C-0), CYBERQUAKE (D-0), NOAH-2D (E-0), DEEPSOIL (J-0 equivalent linear method and J-1, F-0 and M-2, for the non-linear method) NL-DYAS (G-0), OPENSEES (H-0), 1DFD-NL-IM (K-0), ICFEP (L-1), FLAC.7.00 (M-0), DMOD2000 (M-1), GEFDYN (N-0), EPISPEC1D (Q-0), real ESSI (R-0), ASTER (S-0), SCOSSA-1,2 (T-0), SWAP-3C (U-0), GDNL (Y-0), EERA (Z-0) and PLAXIS (Z-1).

The Numerical Scheme

Three types of spatial approximations were considered by the 23 codes used:

1. Finite Element Method: used by 17 teams and implemented in three different ways:
    a. Standard method, used by 17 teams: B-0, C-0, D-0, F-0, H-0, J-0, L-1, M-0, M-2, N-0, R-0, S-0, T-0, U-0 and Z-1.
    b. Spectral method, used by 1 team: Q-0
    c. Galerkin Discontinuous method (GD-FEM), used by 1 team: Y-0.
2. Finite Difference Method, used by 6 teams: A-0, E-0, G-0 and K-0;
3. Analytical solution with equivalent linear method, used by 2 teams: J-1 and Z-0.

The Low Strain Attenuation

For the entire set of codes tested, four kinds of attenuation implementations were used:

1. Frequency-independent attenuation: Applied over a specific frequency bandwidth and considered in the time domain analysis by the use of series of Maxwell/Zener elements: A-0, E-0, F-0, J-0, K-0, J-1, M-0, Q-0 and Z-0.
2. Frequency-dependent attenuation, such as the Rayleigh damping (simplified or full): B-0, G-0, H-0, L-1, M-0, R-0, S-0, T-0, Y-0 and Z-1.
3. Low strain hysteretic damping: C-0, N-0, D-0 and R-0.
4. Numerical damping: U-0, N-0 and D-0

The Non-Linear Constitutive Models

The codes tested here are implemented with various non-linear models, including:

5. IaI model (Iai et al., 2011; Iai and Ozutsumi, 2005): B-0, E-0, Q-0,
6. MKZ modified hyperbolic model (Matasovic and Vucetic, 1993): A-0, T-0
7. Cundall's model (Cundall, 2006): M-0
8. Iwan's model (Iwan, 1967): K-0, U-0, Y-0
9. Logarithmic function model (Puzrin and Shiran, 2000): L-1
10. Modified Hujueux model (Lopez-Caballero et al., 2007): D-0, N-0
11. Multiyield model (Elgamal et al., 2003; Yang et al., 2003): H-0
12. Extended Hyperbolic model (Phillips and Hashash, 2009): F-0, H-0, J-0, M-2
13. Mohr-Coulomb model (Schanz et al., 1999): Z-1
14. Elasto-plastic (Pisanò and Jeremić, 2014): R-0;
15. BWGG: Extented Bouc Wen model (Gerolymos and Gazetas, 2005): G-0
16. Self-developed: C-0

Comparison of Predictions

The participants were asked to give the acceleration and stress-strain time histories at different depths in the soil profile (at ten depths, every 1/10th of the total soil thickness: every 2m for P1, every 10m for P2 and every 5m for P3) in staggered rows: from the very surface for acceleration, and from half the depth interval for stress-strain values. From the "raw" results provided by each participant, a comparative analysis was performed on the computed acceleration time histories, transfer function, 5% pseudo-response spectra, the depth distribution of peak shear strain and PGA, and the stress-strain plots at different depths. Such comparisons were done for each profile, for each computational case (linear vs. non-linear, elastic vs. visco-elastic soil behavior, and rigid vs. elastic substratum conditions) and for the different input motions. For sake of simplicity and conciseness, the main section of the present article only includes results for the P1 case.

Visco-Elastic Computations

For the elastic and visco-elastic computation, most of all results converge towards the analytical solution calculated with the Haskell-Thompson method (Haskell, 1953; Thomson, 1950) after the second iteration. The main discrepancies in amplitude that were corrected in the second iteration came from: (1) the reference motion implementation, (2) units problem, or (3) soil properties implementation. On the other hand, the discrepancy in phase came from the source being located slightly below the sediment/rock interface (for constant time delay). (4) In addition, for the visco-elastic case the convergence was achieved after having specified the reference frequency to be considered. We chose a reference frequency of 4Hz, which is exactly the central frequency of the pulse-like motion

Non-Linear Computations

Once the convergence was achieved for simple cases for which analytical solutions are available, the analysis of the variability of non-linear calculations indicates the variability associated to the implementation of the non-linear soil behavior.

Figure 1 compares the Fourier transfer functions (surface over reference accelerations) of the P1 profile, with a rigid substratum case. Each subplot illustrates the results with the high frequency (HF) waveforms scaled to the lowest PGA (0.5 m/s^2) (a) and largest PGA (5m/s^2) (c) and for the low frequency (LF) waveform scaled to the lowest PGA (0.5 m/s^2) (b) and largest PGA (5m/s^2) (d). The frequency content of the input motion and the scaling of the input motion prove to have a large influence on the non-linear soil behavior in the numerical simulations, and consequently on the dispersion of the results.

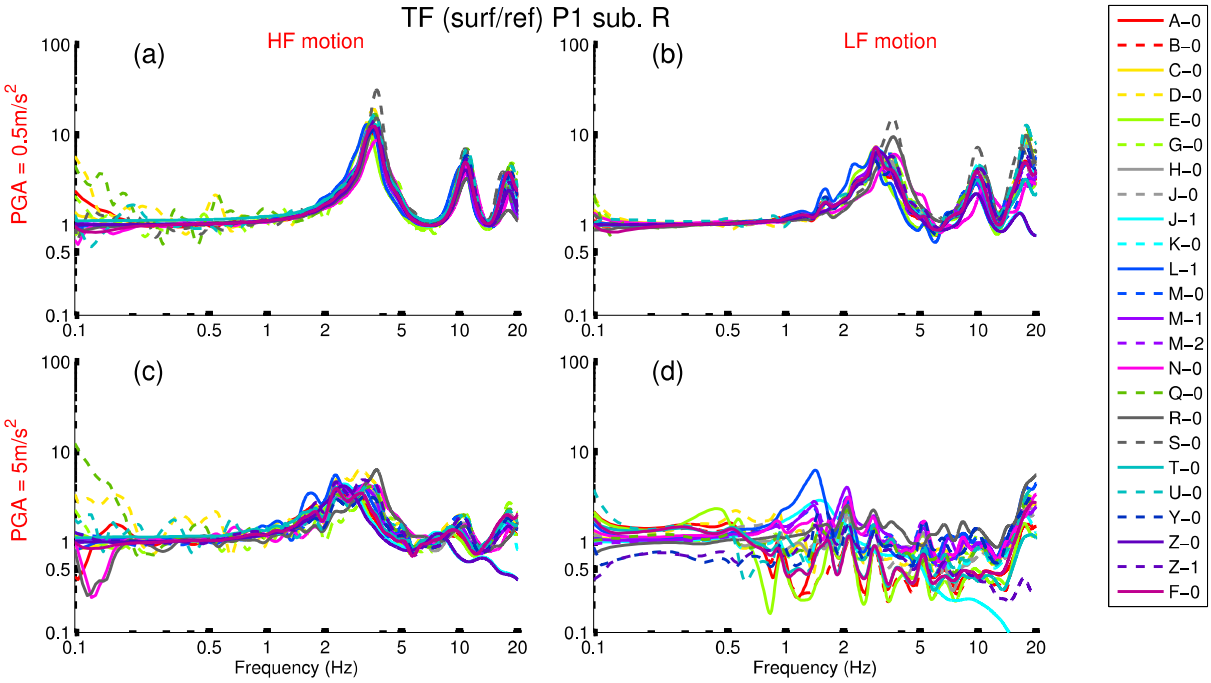

Figure 1: Comparison of the surface to reference Fourier spectra ratio, for the non-linear comparison using for the left sub-graphs the high frequency input motion and for the right sub-graphs the low-frequency input motion and with for the first line the weakest input motion PGA and the second line the highest input motion PGA

Epistemic Uncertainty

Quantification of Result Variability

We quantified the variability between the simulations by the standard deviations in log unit (with base 10) of PGA values, σ_{PGA}. The PGA values at the surface are first compared with the empirical variability (i.e. single station σ_{PGA}). Figure 2 illustrates the σ_{PGA} at the surface of P1 for

the 5 different computational cases. These are the linear–elastic, the linear-visco-elastic, and the non-linear computations with the input motions scaled to the lowest (0.5 m/s^2), medium (1 m/s^2) and highest (5 m/s^2) PGA. The σ_{PGA} is calculated for the pulse-like, the HF and the LF motions. The left subplot gives the results for the rigid substratum, while the right subplot stands for the elastic substratum case.

For the rigid substratum case, σ_{PGA} is greater for the LF than for the HF input motion (around twice greater for the three PGA values), except for the particular linear-elastic case, and σ_{PGA} increases with the PGA for both types of input motions. Similarly, for the elastic substratum case, σ_{PGA} is greater for the LF input motion and increases from linear to non-linear computations as well as with the PGA scaling. The maximum σ_{PGA} observed (0.15) is below the specific single-station σ_{PGA} value for a site with a Vs30 equivalent to P1 (Rodriguez-Marek et al., 2011), which is around 0.2. It suggests that the uncertainties linked with the simulations are themselves below those for the observations.

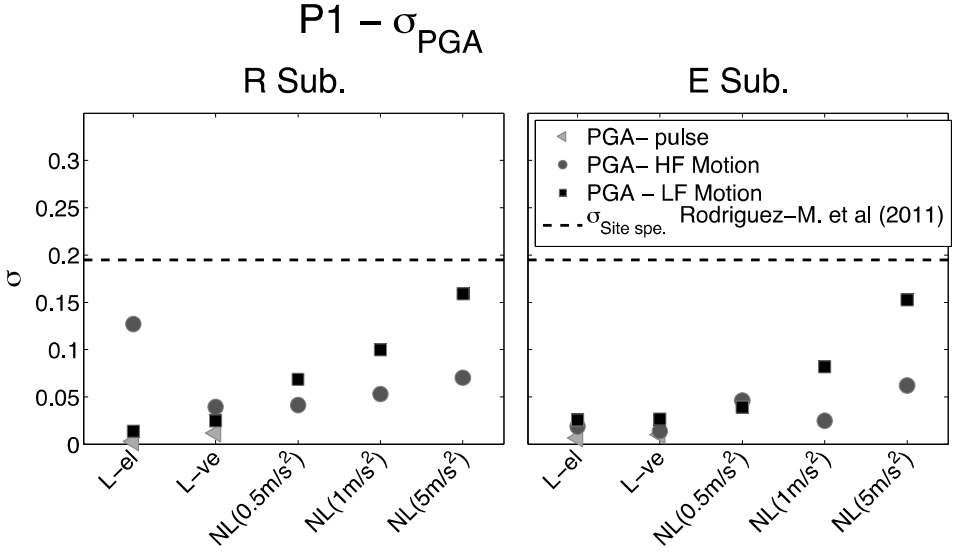

Figure 2: Standard deviation (in log unit) of the PGA at the surface of the profile 1, for the 5 different computational cases (linear –elastic, linear visco-elastic, non-linear with input motion scaled to the lowest (0. 5m/s^2), medium (1 m/s^2) and highest (5 m/s^2) PGA, for the pulse-like, the high frequency and the low frequency content motions. The left sub-graph shows the results for the rigid substratum case and the right sub-graph for the elastic substratum.

Origins of the Variability: Can It Be Reduced?

A priori, we sorted the results into 5 main groups according to the variables implemented in the numerical codes: (G1) attenuation method implemented, (G2) numerical integration scheme, (G3) constitutive model, (G4) use or not of damping control, and (G5) shear strength at the bottom of P1. Each group is further sorted into several sub-groups as follows. We found that G5 and G4 were the most relevant parameters to group the results as the average standard deviation between the results was decreased.

We group the code/team couples into 3 groups: (i) The shear strength (τ_{max}) is constant along the depth and equal to 65kPa and damping control is used (A-0, B-0 and E-0), (ii) τ_{max} is constant equal to 65kPa and damping control is not used (C-0, F-0, G-0, H-0, K-0, Q-0, U-0, Y-O), and (iii) all other teams. Figure 3 compares the pseudo acceleration response spectra at the surface of P1 with a rigid substratum condition subjected to LF and HF input motions and scaled at the medium PGA (1m/s^2) and highest PGA (5m/s^2). The response spectra were sorted according to the previous grouping. The associated standard deviation (σ) is represented by the thin lines at the top of the 4 subplots (the numbers on the right side, indicate the number of code/team couples in each group). This grouping enables the distinction of the response spectra; particularly for the LF input motion. For the LF motion, the σ from the sub-groups (i and ii) with equivalent τ_{max} is reduced below 2s, compared to the rest of the computations (sub-group iii). This period bandwidth is relative to the PGA of this LF input motion. Similarly, for the HF input motion, the σ is reduced below 1 s.

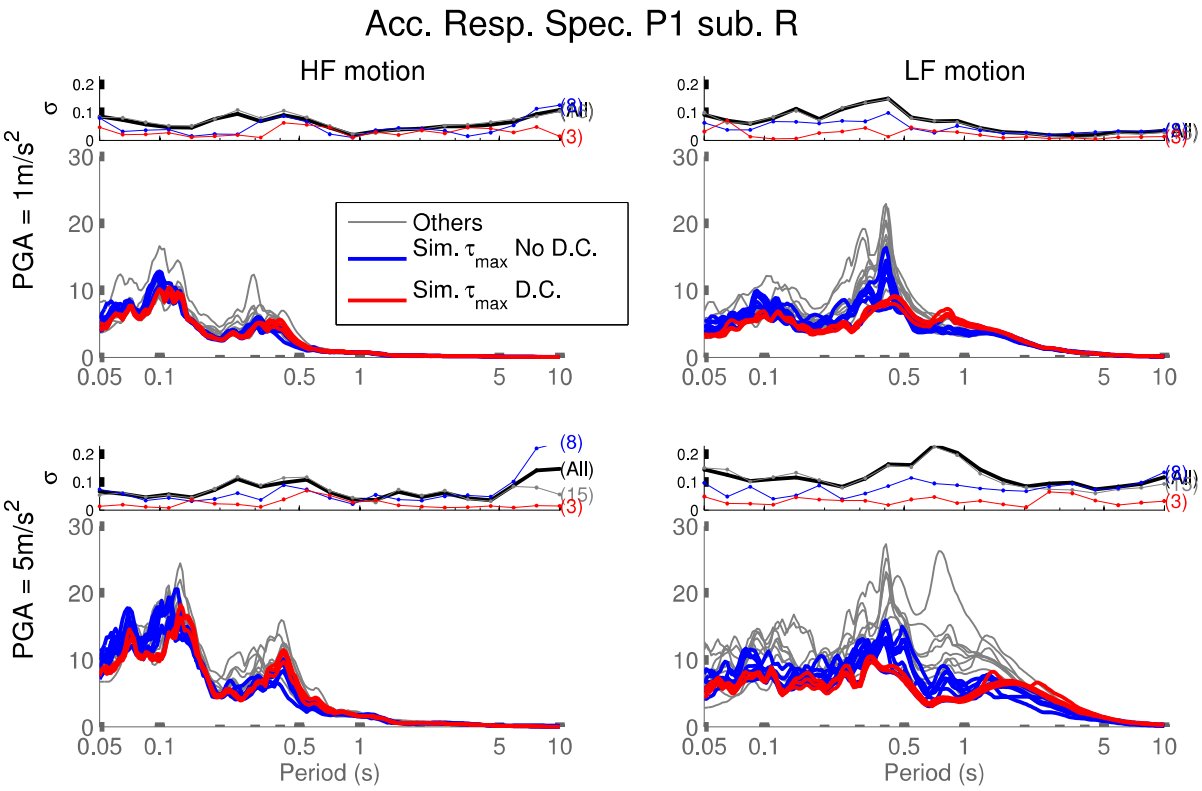

Figure 3: Comparison of the acceleration pseudo-response spectra at the ground surface of P1 with rigid substratum condition, for the non-linear computation. The left sub-graphs are the HF input motion and the right sub-graphs the LF motion. The top subplots are for the medium PGA and the bottom subplots the highest PGA. The response spectra were sorted according to three groups : group 1 is composed of the code/team couples using similar τ_{max} and damping control constitutive model. Group 2 use similar τ_{max} and no damping control and Group 3 are the others code team couples.

Conclusions

In the PRENOLIN's verification phase, the linear computation involving a simple pulse-like (Ricker) input motion proved to be very useful in understanding and eliminating some of the discrepancies between the different numerical codes, which we compared. It was found that code-to-code differences can be attributed to two different sources: (1) different understandings of the expression "input motion" regarding different communities, and (2) different intrinsic attenuation and numerical integration implementations.

The results obtained so far indicate a code-to-code variability, which increases with the shear strain level (which in turn depends on both the PGA level and the frequency content of the reference input motion). We also found that, whatever the soil profiles used (among the 3 soil profiles considered), the overall code-to-code variability in the worst case (with strain levels exceeding 1%) was lower than the random variability of GMPE single-station σ values for PGA.

The effect of different non-linear soil model implementations was explored in this study and our main observations indicate that the epistemic uncertainty (i.e. the code-to-code result variability) can be reduced by describing more precisely certain input parameters, especially the soil shear strength profile. In addition, for one particular non-linear soil model implemented in different codes, the variability of the stress-strain curves were found to be large, and mainly caused by the damping control parameter, which was used or not.

Acknowledgments

We acknowledge the dedicated and proactive participating teams from all over the world: D. Assimaki, J. Shi (Caltech, US), S. Iai (DPRI, Japan), S. Kramer (Univ. Washington, US) E. Foerster (CEA, France), C. Gelis & E. Delavaux (IRSN, France), A.Giannakou (Fugro, France), G. Gazetas E. Garini & N. Gerolymos (NTUA, Greece), J. Gingery (UCSD, US), Y. Hashash & J. Harmon (Univ, Illinois), P. Moczo, J.Kristek & A. richterova (CUB, Slovakia), S. Foti & S. Kontoe (Politecnico di Torino & Imperial college, Italy) G. Lanzo (Univ. Rome La Sapienza, Italy) F. Lopez-Caballero & S. Montoya-Noguera (ECP, France), F. De-Martin (BRGM, France), B. Jeremic, F. Pisano & K. Watanabe (UCD, TU Delft & Shimizu Corp, US), A. Nieto-Ferro (EDF, France), A. Chiaradonna, F. Silvestri & G. Tropeano (UNICA, Italy), MP-Santisi d'Avila (UNS, Nice) D. Mercerat (CEREMA, France) and D. Boldini (UNIBO, Italie)

References

Cundall, P., 2006. A simple hysteretic damping formulation for dynamic continuum simulations, in: *Proceedings of the 4th International FLAC Symposium on Numerical Modeling in Geomechanics*. Minneapolis: Itasca Consulting Group.

Elgamal, A., Yang, Z., Parra, E., Ragheb, A., 2003. Modeling of cyclic mobility in saturated cohesionless soils. Int. *J. Plast*. **19**, 883 – 905. doi:http://dx.doi.org/10.1016/S0749-6419(02)00010-4

Gerolymos, N., Gazetas, G., 2005. Constitutive model for 1-D cyclic soil behaviour applied to seismic analysis of layered deposits. *Soils Found*. **45**, 147–159.

Haskell, N.H., 1953. The dispersion of surface waves in multilayered media. *Bull. Seismol. Soc. Am.* **43**, 17–34.

Iai, S., Ozutsumi, O., 2005. Yield and cyclic behaviour of a strain space multiple mechanism model for granular

materials. *Int. J. Numer. Anal. Methods Geomech.* **29**, 417–442. doi:10.1002/nag.420

Iai, S., Tobita, T., Ozutsumi, O., Ueda, K., 2011. Dilatancy of granular materials in a strain space multiple mechanism model. *Int. J. Numer. Anal. Methods Geomech*. **35**, 360–392. doi:10.1002/nag.899

Iwan, W.D., 1967. On a class of models for the yielding behavior of continuous and composite systems. *J. Appl. Mech*. **34**, 612–617.

Kwok, A.O., Stewart, J.P., Hashash, Y.M., 2008. Nonlinear ground-response analysis of Turkey Flat shallow stiff-soil site to strong ground motion. *Bull. Seismol. Soc. Am*. **98**, 331–343.

Lopez-Caballero, F., Razavi, A.M.-F., Modaressi, H., 2007. Nonlinear numerical method for earthquake site response analysis I—elastoplastic cyclic model and parameter identification strategy. *Bull. Earthq. Eng*. **5**, 303–323.

Matasovic, N., vucetic, M., 1993. Analysis of seismic records obtained on november 24, 1987 at the Wildlife liquefaction array. University of California, Los Angeles.

Olsen, K., Day, S., Bradley, C., 2003. Estimation of Q for long-period (> 2 sec) waves in the Los Angeles basin. *Bull. Seismol. Soc. Am*. **93**, 627–638.

Phillips, C., Hashash, Y.M.A., 2009. Damping formulation for nonlinear 1D site response analyses. *Soil Dyn. Earthq. Eng*. **29**, 1143 – 1158. doi:http://dx.doi.org/10.1016/j.soildyn.2009.01.004

Pisanò, F., Jeremić, B., 2014. Simulating stiffness degradation and damping in soils via a simple visco-elastic–plastic model. *Soil Dyn. Earthq. Eng*. **63**, 98–109.

Puzrin, A.M., Shiran, A., 2000. Effects of the constitutive relationship on seismic response of soils. Part I. Constitutive modeling of cyclic behavior of soils. *Soil Dyn. Earthq. Eng.* **19**, 305 – 318. doi:http://dx.doi.org/10.1016/S0267-7261(00)00027-0

Rodriguez-Marek, A., Mantalva, G. 1, Cotton, F., Bonilla, F., 2011. Analysis of Single-Station Standard Deviation Using the KiK-net Data. *Bull. Seismol. Soc. Am*. **101**, 1242–1258.

Schanz, T., Vermeer, P.A., Bonnier, P.G., 1999. The hardening soil model: formulation and verification. 2000 *Comput. Geotech*. 281–296.

Stewart, J., Kwok, A., 2009. Nonlinear Seismic Ground Response Analysis: Protocols and VerificaBon Against Array Data. PEER Annu. Meet. San Franc.-Present. 84.

Thomson, W.T., 1950. Transmission of elastic waves through a stratified solid. *J. Appl. Phys*. **21**, 89–93.

Yang, Z., Elgamal, A., Parra, E., 2003. Computational model for cyclic mobility and associated shear deformation. *J. Geotech. Geoenvironmental Eng*. **129**, 1119–1127.